

RESEARCH ARTICLE

Juvenile hormone acts through FoxO to promote *Cdc2* and *Orc5* transcription for polyploidy-dependent vitellogenesis

Zhongxia Wu*, Qiongjie He*, Baojuan Zeng, Haodan Zhou and Shutang Zhou[‡]

ABSTRACT

Vitellogenin (Vg) is a prerequisite for egg production and embryonic development after ovipositioning in oviparous animals. In many insects, juvenile hormone (JH) promotes fat body cell polyploidization for the massive Vg synthesis required for the maturation of multiple oocytes, but the underlying mechanisms remain poorly understood. Using the migratory locust *Locusta migratoria* as a model system, we report here that JH induces the dephosphorylation of Forkhead box O transcription factor (FoxO) through a signaling cascade including leucine carboxyl methyltransferase 1 (LCMT1) and protein phosphatase 2A (PP2A). JH promotes PP2A activity via LCMT1-mediated methylation, consequently triggering FoxO dephosphorylation. Dephosphorylated FoxO binds to the upstream region of two endocycle-related genes, *cell-division-cycle 2* (*Cdc2*) and *origin-recognition-complex subunit 5* (*Orc5*), and activates their transcription. Depletion of *FoxO*, *Cdc2* or *Orc5* results in blocked polyploidization of fat body cells, accompanied by markedly reduced Vg expression, impaired oocyte maturation and arrested ovarian development. The results suggest that JH acts via LCMT1-PP2A-FoxO to regulate *Cdc2* and *Orc5* expression, and to enhance ploidy of fat body cells in preparation for the large-scale Vg synthesis required for synchronous maturation of multiple eggs.

KEY WORDS: Juvenile hormone, FoxO, Fat body, Endocycle, Vitellogenesis

INTRODUCTION

Arthropod-specific juvenile hormone (JH), a sesquiterpenoid produced in corpora allata, governs insect metamorphosis and reproduction. During the pre-metamorphic stage, JH acts as an anti-metamorphic hormone to maintain the larval/nymphal characteristics of insects by suppressing the steroid hormone 20-hydroxyecdysone (20E)-induced larva-pupa or nymphal-adult transition (Jindra et al., 2013; Riddiford, 1994). In adulthood, JH acts as a gonadotrophic hormone to stimulate various aspects of female reproduction, including previtellogenic development, vitellogenesis and oocyte maturation (Raikhel et al., 2005; Roy et al., 2018). Cumulative studies have established that JH exerts its genomic action via inducing the heterodimerization of Methoprene-tolerant (Met) and Taiman (Tai) to form a JH-receptor

complex, consequently activating the transcription of JH-responsive genes (Charles et al., 2011; Guo et al., 2014; Jindra et al., 2015; Kayukawa et al., 2012; Li et al., 2011; Wang et al., 2017). In addition, JH acts via the RTK-PLC-IP3-CaMKII signaling cascade to trigger the phosphorylation of Met for enhanced transcriptional activity in the mosquito *Aedes aegypti* (Liu et al., 2015; Ojani et al., 2016). Moreover, JH, through the RTK-PI3K-Akt signaling pathway, stimulates the phosphorylation of serine/arginine-rich (pre-mRNA) splicing factor (SRSF) to induce the alternative splicing of Tai (Liu et al., 2018). The produced Tai-A and Tai-B isoforms potentiate the transcriptional activity of 20E-receptor in the fat body of adult female mosquitoes essential for blood meal-induced vitellogenesis and egg production (Liu et al., 2018). In the cotton bollworm *Helicoverpa armigera*, JH acts on the phosphorylation of the pupal specifier Broad-complex (Br-C) to repress 20E-initiated metamorphosis via the GPCR-PLC-PKC pathway (Cai et al., 2014). In the migratory locust *Locusta migratoria*, JH elicits the phosphorylation and activation of Na⁺/K⁺-ATPase via a signaling cascade of GPCR/RTK-PLC-IP3R-PKC, facilitating the initiation of intercellular channels (known as patency) in the follicular epithelium to accelerate the transportation of yolk protein precursor, vitellogenin (Vg) (Jing et al., 2018). Although the mode of JH action in suppressing larval metamorphosis has been well studied (Jindra et al., 2013; Li et al., 2019), the molecular basis of JH in promoting adult reproduction has received much less attention (Li et al., 2019; Roy et al., 2018; Santos et al., 2019).


A hallmark of female insect reproduction is vitellogenesis, a process by which Vg is synthesized in the fat body, transported through hemolymph and sequestered into developing oocytes. Vitellogenesis is prerequisite of insect egg production and embryonic growth after oviposition. JH-dependent vitellogenesis has been reported in a variety of insect species, from the hemimetabolous *L. migratoria* to the basal order of holometabolous insects such as the beetle *Tribolium castaneum*, as well as the more advanced dipteran insects such as *Drosophila melanogaster* (Belles, 2004; Raikhel et al., 2005; Roy et al., 2018; Wyatt and Davey, 1996). *L. migratoria*, which bears panoistic and synchronously matured oocytes, has been a long-standing model for studying JH-dependent reproduction (Raikhel et al., 2005; Roy et al., 2018; Wyatt and Davey, 1996). In *L. migratoria*, JH acts independently of 20E to promote vitellogenesis, oogenesis and egg maturation (Belles, 2004; Raikhel et al., 2005; Song et al., 2013, 2019). During the first gonadotrophic cycle of locusts, the fat body, homologue of vertebrate liver and adipose tissue, undergoes endocycling to produce up to 32C (chromatin-value) polyploid cells (Guo et al., 2014; Wu et al., 2016, 2018). The polyploidization of fat body cells in adult female locusts is induced by JH, which facilitates the massive synthesis of Vg and possibly other proteins required for multiple egg production (Guo et al., 2014; Wu et al., 2016, 2018). However, the regulatory mechanisms of polyploidization regulated by JH remain poorly understood.

Polyploidy, which is commonly seen throughout plants and animals, is generated by repeated gap (G)-synthesis (S) cycles

Key Laboratory of Plant Stress Biology, State Key Laboratory of Cotton Biology, School of Life Sciences, Henan University, Kaifeng 475004, China.

*These authors contributed equally to this work

[‡]Author for correspondence (szhou@henu.edu.cn)

 Z.W., 0000-0002-9685-8452; B.Z., 0000-0001-8139-2082; H.Z., 0000-0002-8612-4404; S.Z., 0000-0003-4881-3644

This is an Open Access article distributed under the terms of the Creative Commons Attribution License (<https://creativecommons.org/licenses/by/4.0/>), which permits unrestricted use, distribution and reproduction in any medium provided that the original work is properly attributed.

Handling Editor: Cassandra Extavour
Received 28 January 2020; Accepted 20 July 2020

without mitotic (M) phase (Edgar and Orr-Weaver, 2001; Edgar et al., 2014; Orr-Weaver, 2015; Zielke et al., 2013). In insects, polyploidy is widespread in highly metabolic tissues such as the fat body, ovary, midgut, salivary gland, prothoracic gland and wing imaginal discs (Buntrock et al., 2012; Jacobson et al., 2013; Nordman and Orr-Weaver, 2012; Ohhara et al., 2017). Although polyploidy is essential for insect development, metamorphosis and reproduction, the regulatory mechanisms of polyploidization in JH-dependent reproduction remain elusive (Koyama et al., 2004; Li and White, 2003; Moriyama et al., 2016; Sun et al., 2008). Our previous investigation showed that JH upregulated the expression of 16 genes associated with DNA replication and 13 genes involved in cell cycle progression (Guo et al., 2014). Of these, the chromosome maintenance (Mcm) genes *Mcm3*, *Mcm4* and *Mcm7*, as well as *cell-division-cycle 6* (*Cdc6*), *cyclin-dependent kinase 6* (*Cdk6*) and *adenovirus E2 factor-1* (*E2f1*), were expressed in response to both JH and its receptor Met (Guo et al., 2014). Moreover, the JH-Met/Tai receptor complex bound to the upstream of *Mcm4*, *Mcm7*, *Cdc6*, *Cdk6* and *E2f1*, and activated their transcription for polyploidization (Guo et al., 2014; Wu et al., 2016, 2018). Notably, *Met* RNAi had no significant effect on other genes that were upregulated by JH, suggesting that other signaling cascades that interplay with JH are likely involved in JH-dependent polyploidization. The crosstalk of JH and insulin (or insulin-like peptide, ILP) pathways has been reported in insect development and reproduction (Gruntenko and Rauschenbach, 2018; Mirth et al., 2014; Sheng et al., 2011; Sim and Denlinger, 2013). Here, we show previously unidentified evidence that JH stimulates FoxO dephosphorylation through leucine carboxyl methyltransferase 1 (LCMT1)-mediated activation of protein phosphatase 2A (PP2A). FoxO activates the transcription of *cell-division-cycle 2* (*Cdc2*) and *origin-recognition-complex subunit 5* (*Orc5*), consequently stimulating fat body cell polyploidization and massive Vg synthesis to meet the requirement of multiple oocyte maturation and egg production.

RESULTS

JH induces FoxO dephosphorylation during locust vitellogenesis

The first gonadotrophic cycle of adult female locusts under this study was about 9-10 days. According to *Vg* transcript level and terminal

oocyte length, the adult females underwent previtellogenesis from 0 to 4 days post adult eclosion (PAE) and vitellogenesis started from approximately day 4-5. We first collected the fat body of adult females during 0-7 days PAE to reveal the dynamics of *FoxO* expression via qRT-PCR. As shown in Fig. 1A, no significant change of *FoxO* mRNA abundance was observed. We next conducted qRT-PCR using total RNA from the fat bodies of 10-day-old adult females that had been treated with precocene for 10 d, some of which were further treated with methoprene for 6-48 h. Neither chemical ablation of endogenous JH by precocene treatment nor additional application of JH analogue significantly changed *FoxO* transcript levels (Fig. 1B). We further performed western blots to examine the temporal abundance of FoxO proteins. A polyclonal anti-FoxO antibody was raised, and its specificity was determined together with a commercial antibody against the phosphorylated FoxO (p-FoxO) by western blot analysis of *FoxO*-depleted versus dsGFP-treated fat bodies (Fig. S1). As shown in Fig. 1C, the protein levels of FoxO had no apparent change during 0-7 days PAE, mirroring the lack of change in mRNA levels. Interestingly, p-FoxO abundance was extremely low within 12 h of adult emergence (0 day PAE), then gradually elevated and reached a peak at 3 days PAE, but declined starting from 4 days PAE (Fig. 1C). We previously reported that hemolymph JH titers were undetectable at adult female eclosion, progressively elevated in previtellogenic phase, sharply increased in early vitellogenic stage and rose to a peak in the late vitellogenic stage (Fig. 1C) (Guo et al., 2019). Because adult female locusts started feeding 12 h post-eclosion, the extremely low p-FoxO levels within 12 h of adult emergence might be primarily due to the absence of food intake. Likewise, the enhanced levels of p-FoxO during the previtellogenic phase suggest an upregulation by nutrient-induced activation of ILP signaling, along with low level of JH titers. The subsequent reduction of p-FoxO levels during the vitellogenic stage may imply a link between FoxO dephosphorylation and the high level or a peak of JH titers in this duration. To confirm the responsiveness of FoxO dephosphorylation to JH, we performed western blotting using the protein extracts from a fat body from 10-day-old adult females, adult females treated with precocene for 10 days as well as those further treated with methoprene for 6-48 h. As shown in Fig. 1D, p-FoxO abundance was extremely low in precocene-treated adult females, similar to that in 10-day-old adult females. It should be

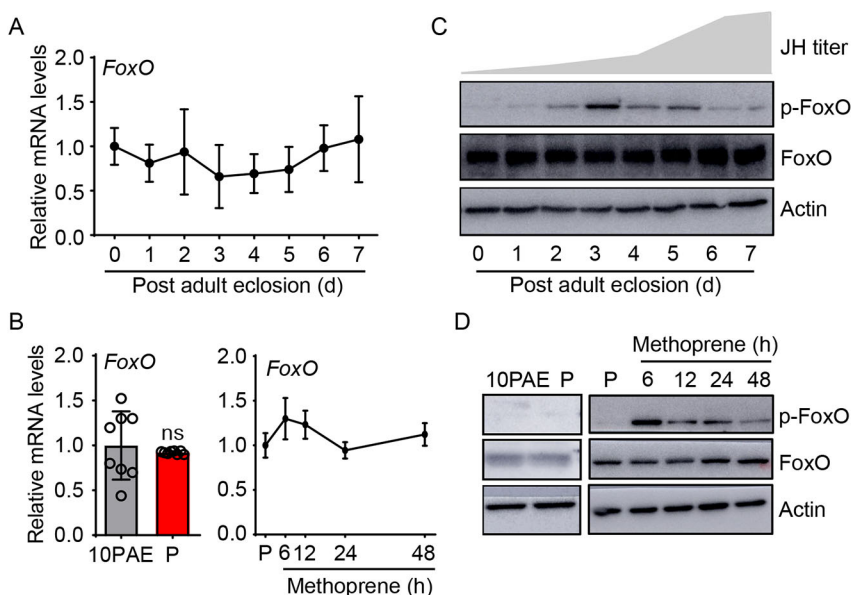


Fig. 1. Induction of FoxO dephosphorylation by JH. (A) qRT-PCR showing the developmental profile of *FoxO* mRNA in the fat body of adult females from 12 h after adult emergence (0 day) to 7 days post adult eclosion ($n=8$). (B) Relative *FoxO* mRNA levels in the fat body of 10-day-old adult females (10PAE), precocene-treated adult females for 10 days (P) and those further treated with methoprene for 6-48 h. ns, no significant difference ($n=8$). (C) Western blots showing the dynamics of total FoxO (FoxO) and phosphorylated FoxO (p-FoxO) in the fat body of adult females on day 0-7. (D) The levels of FoxO and p-FoxO in the fat body of 10-day-old adult females (10PAE), precocene-treated adult females for 10 days (P) and further treated with methoprene for 6-48 h.

noted that precocene was applied to adult females within 12 h of eclosion. The data indicate the involvement of other factors in regulating FoxO phosphorylation in JH-deprived adult females. Interestingly, p-FoxO abundance increased at 6 h but declined 12–48 h post methoprene treatment (Fig. 1D). These observations suggest that short-term exposure of JH-deprived adult females to exogenous JH may activate signaling cascades triggering FoxO phosphorylation, whereas prolonged treatment of JH stimulates FoxO dephosphorylation.

JH induces FoxO dephosphorylation via LCMT1-PP2A signaling cascade

FoxO is known to be directly phosphorylated by Akt (or protein kinase B, PKB) and dephosphorylated by PP2A (Singh et al., 2010). Akt is activated by active insulin signaling through phosphorylation mediated by the PI3K-PIP3-PDK axis (Manning and Toker, 2017). PP2A methylation at residue Leu309 of catalytic subunit triggers its activation (Sents et al., 2013; Sontag et al., 2013), whereas PP2A phosphorylation at residues Tyr307 and Thr304 of the catalytic subunit inhibits its activity (Janssens and Goris, 2001; Janssens et al., 2008; Sents et al., 2013; Sontag et al., 2013). As shown in Fig. 2A, the levels of Akt and phosphorylated Akt (p-Akt) increased from 0 to 3 days PAE. However, no apparent change was observed in p-Akt levels on day 4–7 (Fig. 2A). The results suggest that the reduced levels of p-FoxO during vitellogenic stage (Fig. 1C) is unlikely caused by a decline of Akt activity in this period. With respect to phosphorylated PP2A (p-PP2A), its levels had no conspicuous change at 1–7 days PAE (Fig. 2A). Furthermore, no obvious change was seen in p-Akt or p-PP2A levels 6–48 h post methoprene treatment (Fig. 2B). This pattern is different from the fluctuation of p-FoxO levels upon methoprene application (Fig. 1D). Collectively, these results suggest that neither p-Akt

nor p-PP2A is involved in the reduction of p-FoxO levels during vitellogenic stage.

We next performed a series of experiments to determine whether methylated PP2A (m-PP2A) contributed to the reduced levels of p-FoxO during *L. migratoria* vitellogenesis. PP2A knockdown or PP2A inhibitor (okadaic acid, OA) treatment led to substantially reduced levels of m-PP2A in the fat body (Fig. 2C). Consequently, the catalytic activity of PP2A significantly declined (Fig. 2D). As a result, the abundance of p-FoxO was significantly elevated whereas FoxO levels remained constant (Fig. 2E and Fig. S2A B). In contrast, PP2A knockdown or OA treatment had no obvious effect on Akt or p-Akt abundance (Fig. 2F), suggesting that PP2A-dependent dephosphorylation of FoxO is unlikely to be mediated by Akt. As shown in Fig. 3A, m-PP2A abundance in the fat body substantially increased on day 4 and remained high at 5–7 days PAE (Fig. 3A). A similar pattern was seen with PP2A activity measured by ELISA (Fig. 3B). When endogenous JH was eliminated by chemical allatectomy, PP2A methylation was blocked (Fig. 3C). Further application of methoprene restored PP2A methylation, and m-PP2A reached high levels at 24–48 h post methoprene treatment (Fig. 3C). In contrast, PP2A had no noticeable change at its total protein levels (Fig. 3C). Accordingly, PP2A activity significantly decreased in JH-deprived fat bodies compared with that at 10 days PAE, but was significantly increased after methoprene treatment (Fig. 3D). Taken together, these observations indicate that JH induces PP2A methylation and consequently promotes PP2A activity. Moreover, depletion of PP2A resulted in lower cell ploidy and substantial reduction of *Vg* expression in the fat body, accompanied by blocked ovarian growth and arrested oocyte maturation (Fig. S3A–D). Notably, the capacity of methoprene to induce FoxO dephosphorylation was blocked by PP2A knockdown (Fig. S3E).

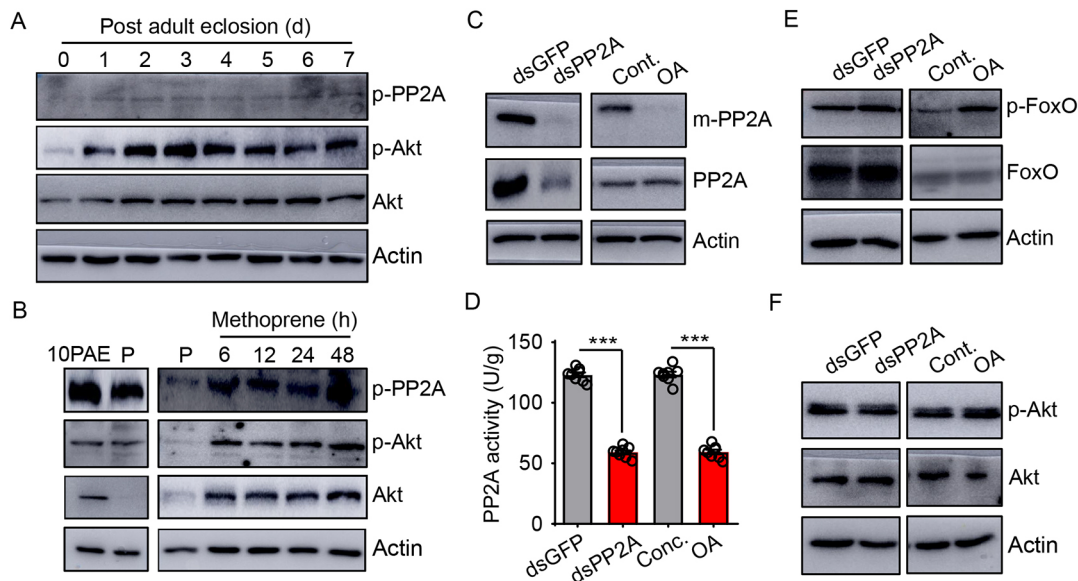


Fig. 2. FoxO dephosphorylation triggered by PP2A methylation and activation. (A) Developmental profiles of total Akt protein (Akt), phosphorylated Akt (p-Akt) and phosphorylated PP2A (p-PP2A) in the fat body of adult females on day 0–7. (B) The abundance of Akt, p-Akt and p-PP2A in the fat body of 10-day-old adult females (10PAE), precocene-treated adult females for 10 days (P) and those further treated with methoprene for 6–48 h. (C) Left panel showing the change of total PP2A protein (PP2A) and methylated PP2A (m-PP2A) in the fat body of adult females treated with dsPP2A versus dsGFP controls. Right panel showing the change of PP2A and m-PP2A in the fat body of adult females treated with PP2A inhibitor, okadaic acid (OA), compared with the DMSO solvent control (Cont.). (D) PP2A activity measured by ELISA in the fat body of adult females treated with dsPP2A, OA, dsGFP and DMSO, respectively. *** $P < 0.001$; $n = 8$ (Student's *t*-test). (E) The levels of FoxO and p-FoxO in the fat body of adult females subjected to dsPP2A, dsGFP, OA and DMSO treatment. (F) The abundance of Akt and p-Akt in the fat body of adult females treated with dsPP2A, dsGFP, OA and DMSO.

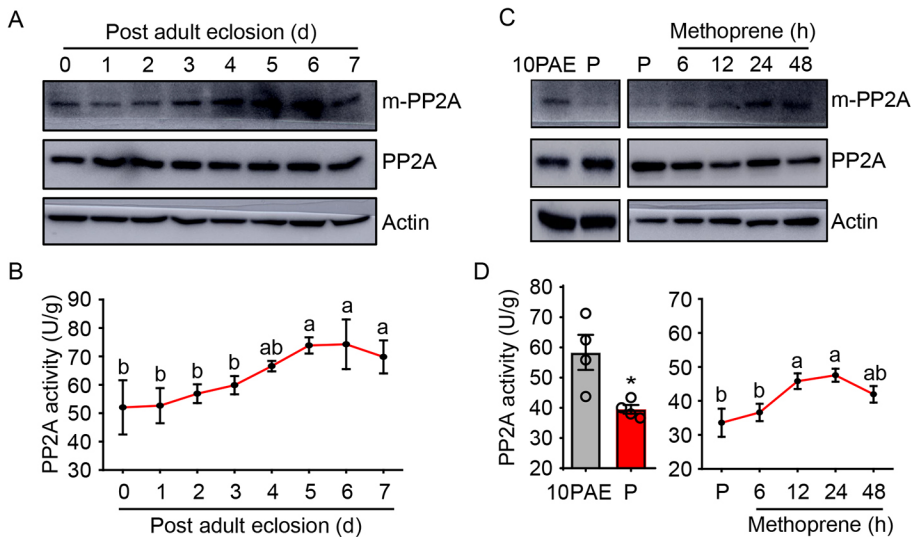


Fig. 3. Induction of PP2A methylation and activation by JH. (A) Developmental dynamics of PP2A and m-PP2A in the fat body of adult females on day 0 to 7. (B) PP2A activity in the fat body of adult females on day 0 to 7. Means labeled with different letters indicate significant difference at $P < 0.05$ ($n=3$) (ANOVA with Tukey's post-hoc test). (C) The levels of PP2A and m-PP2A in the fat body of 10-day-old adult females (10PAE), precocene-treated adult females for 10 days (P) and those further treated with methoprene for 6–48 h. (D) PP2A activity in the fat body of 10-day-old adult females (10PAE), precocene-treated adult females for 10 days (P) and those further treated with methoprene for 6–48 h. Left panel, $*P < 0.05$ ($n=3$) (Student's *t*-test). Right panel, means labeled with different letters indicate significant difference at $P < 0.05$ ($n=3$) (ANOVA with Tukey's post-hoc test).

As PP2A methylation is specifically catalyzed by LCMT1 (Sents et al., 2013; Sontag et al., 2013), we next investigated the effect of *LCMT1* RNAi on PP2A activity and FoxO dephosphorylation. A polyclonal anti-LCMT1 antibody was raised and its specificity was verified by western blotting using *LCMT1*-depleted versus dsGFP-treated fat bodies (Fig. S4). When *LCMT1* was depleted (Fig. 4A), both m-PP2A abundance and PP2A activity were significantly reduced, whereas PP2A protein levels remained unchanged (Fig. 4B,C). Consequently, p-FoxO abundance was significantly elevated (Fig. 4D and Fig. S5). Because of experiment-to-experiment variation, different band intensity of p-FoxO in western blots was seen in the fat body of adult females on day 7–10 (Figs 1C, 2E and 4D). The observations also suggest the fluctuation of p-FoxO levels in the fat body of adult females from 7 to 10 days PAE. As shown in Fig. 4E and Fig. S6A, *LCMT1* protein but not mRNA levels significantly increased after adult eclosion. Neither precocene nor methoprene treatment had a significant effect on *LCMT1* mRNA level (Fig. S6B and S6C). However, deprivation of JH resulted in markedly reduced levels of *LCMT1* protein, and additional methoprene treatment led to increased levels of *LCMT1* protein (Fig. 4F). The above data together indicate that JH induces *LCMT1* protein expression, which in turn promotes PP2A methylation and phosphatase activity, consequently triggering FoxO dephosphorylation. Furthermore, *LCMT1* knockdown

resulted in lower cell ploidy and remarkable reduction of *Vg* expression in the fat body along with blocked ovarian growth and arrested oocyte maturation (Fig. S7A–D). The capacity of methoprene to induce FoxO dephosphorylation was also blocked by *PP2A* knockdown (Fig. S7E).

FoxO knockdown blocks polyploidization, vitellogenesis and oocyte maturation

Knowing that FoxO dephosphorylation was induced by JH through *LCMT1*-dependent PP2A methylation, we next defined the role of FoxO in JH-stimulated polyploidization, vitellogenesis, oocyte maturation and ovarian development. *FoxO* RNAi caused 67% reduction of its normal transcript abundance and substantial decline of its protein levels in the fat body of adult females at 8 days PAE (Fig. 5A). Knocking down *FoxO* resulted in lower ploidy and smaller nuclei of fat body cells (Fig. 5B). Quantitative analysis of ploidy by flow cytometry showed that distinct from the peaks at 8C and 16C in the dsGFP controls, a 2C peak with small populations of 8C and 16C was observed with *FoxO*-depleted fat bodies of adult females at 8 days PAE (Fig. 5C). Silencing of *FoxO* reduced *VgA* (GenBank KF171066) and *VgB* (GenBank KX709496) mRNA levels to 6% and 4% of the dsGFP controls (Fig. 5D). The protein levels of *VgA* and *VgB* were also markedly decreased (Fig. 5D). Concurrently, the primary oocytes and ovaries of *FoxO*-depleted

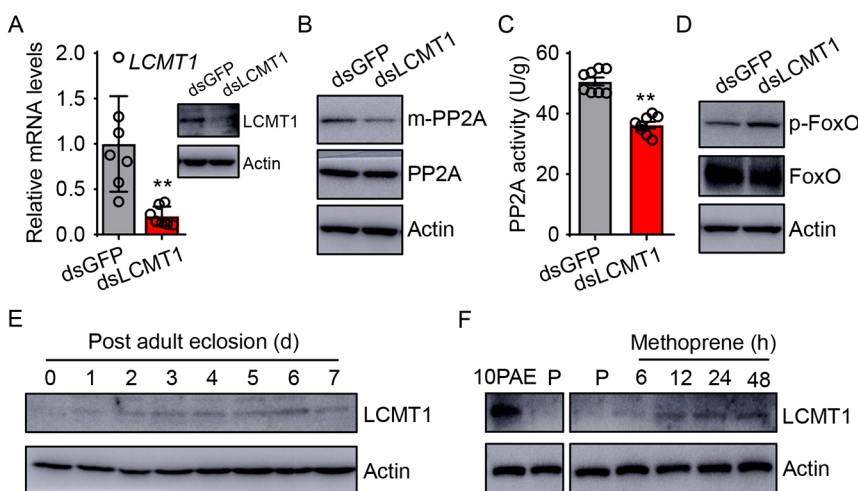


Fig. 4. *LCMT1* responsiveness to JH and effect on PP2A activity and FoxO dephosphorylation. (A) qRT-PCR and western blot showing *LCMT1* RNAi efficiency in the fat body of adult females at 8 days post adult eclosion. $**P < 0.01$ compared with the dsGFP control ($n=8$) (Student's *t*-test). (B) The levels of PP2A and m-PP2A in the fat body of adult females subjected to ds*LCMT1* and dsGFP treatment. (C) PP2A activity in the fat body of adult females treated with ds*LCMT1* and dsGFP. $**P < 0.01$ compared with the dsGFP control ($n=8$) (Student's *t*-test). (D) The levels of FoxO and p-FoxO in the fat body of adult females treated with ds*LCMT1* versus dsGFP controls. (E) Developmental profiles of *LCMT1* in the fat body of adult females on day 0 to 7. (F) The levels of *LCMT1* in the fat body of 10-day-old adult females (10PAE), precocene-treated adult females for 10 days (P) and those further treated with methoprene for 6–48 h.

adult females were obviously smaller than that of dsGFP controls on day 8 (Fig. 5E). Statistically, the length \times width index of primary oocytes of *FoxO*-depleted locusts was 4.9, whereas that of dsGFP controls was 8.0 (Fig. 5F). Collectively, these data imply a crucial role of *FoxO* in fat body cell polyploidization and oocyte maturation.

FoxO directly activates the transcription of *Cdc2* and *Orc5*

We have previously reported that JH upregulated the expression of 29 genes associated with cell polyploidization in locust fat body, but *Met* RNAi only reduced the expression of *Mcm3*, *Mcm4*, *Mcm7*, *Cdc6*, *Cdk6* and *E2f1* (Guo et al., 2014; Wu et al., 2016, 2018). To explore the involvement of FoxO, we examined the effect of *FoxO* knockdown on the expression of other 23 genes. Three genes, including *Cdc2* (also known as *Cyclin-dependent kinase 1*, *Cdk1* in mammals), *Orc5* and *Replication protein A2* (*RFA2*), showed a reduction in transcript levels upon *FoxO* knockdown (Fig. S8). Analysis of a 3 kb upstream sequence of *Cdc2* revealed a conserved FoxO response element (FRE; GTAAATAA) in the promoter region (nucleotides -1286 to -1279) (Fig. 6A), which has been previously documented for FoxO binding and transcriptional gene regulation in insects (Cai et al., 2016; Luo et al., 2007; Mahoney et al., 2016; Zeng et al., 2017; Zhang et al., 2016). This FRE was also seen in the promoter of *Orc5* gene (nucleotides -818 to -811) (Fig. 6A). However, no FRE was found in the promoter of *RFA2*. We therefore concentrated our efforts on *Cdc2* and *Orc5*. We exogenously expressed locust FoxO in *Drosophila* S2 cells (Fig. 6B), and next conducted luciferase reporter assays and EMSA to determine the transcriptional regulation of *Cdc2* and *Orc5* by FoxO. In the luciferase reporter assays, the upstream regulatory

sequences of *Cdc2* (nucleotides -1912 to -1014) or *Orc5* (nucleotides -1115 to -46) containing the FoxO-binding site were cloned into the pGL4.10 vector and co-transfected with pAc5.1/Flag-FoxO or pAc5.1/Flag empty vector into S2 cells. The pAc5.1/Flag empty vector was used as the control. As shown in Fig. 6C,D, ectopic expression of locust FoxO led to significant increase of *Cdc2* and *Orc5* reporter activities compared with the empty controls. To further characterize the binding of FoxO to FRE in *Cdc2* and *Orc5* promoters, we performed EMSA using nuclear extracts from S2 cells transfected with pAc5.1/Flag-FoxO and 20-mer nucleotide probes corresponding to the sequences containing the FRE in *Cdc2* and *Orc5* promoters (Fig. 6A). As shown in Fig. 6E,F, the specific bands were detected with biotin-labeled *Cdc2* and *Orc5* probes (lanes 2 and 5). These specific bands were abolished after a 200 \times molar excess of the unlabeled *Cdc2* and *Orc5* probes (lanes 3) or their mutated biotin-labeled probes (lanes 4) were added into the reaction (Fig. 6E,F). Pre-incubation of cell nuclear extracts with anti-Flag antibody (lanes 6) resulted in the elimination of specific bands, whereas pre-incubation with IgG (lanes 7) had no apparent effect on their mobility or intensity (Fig. 6E,F). Together, these observations indicate that FoxO binds to *Cdc2* and *Orc5* promoters, and stimulates their transcription.

Depletion of *Cdc2* and *Orc5* phenocopies *FoxO* knockdown

Cdc2 RNAi caused 50.9% reduction of its normal mRNA levels in the fat body of adult females at 8 days PAE (Fig. 7A). In respect of *Orc5* RNAi, the mRNA levels of *Orc5* were reduced by 67% (Fig. 7A). As in the case of *FoxO* knockdown, both *Cdc2*- and *Orc5*-depleted fat bodies had markedly lower ploidy and small nuclei compared with the dsGFP controls (Fig. 7B). In comparison

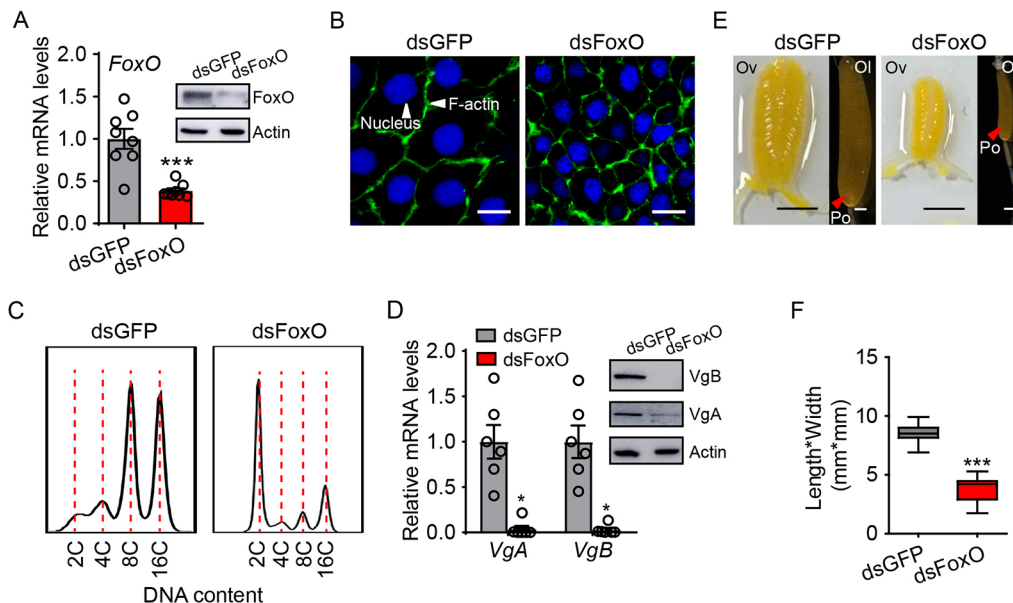


Fig. 5. Effect of *FoxO* knockdown on fat body cell polyploidization and vitellogenesis. (A) Relative mRNA and protein levels showing *FoxO* RNAi efficiency in the fat body of females at 8 days post adult eclosion. *** $P < 0.001$ compared with the dsGFP control ($n=8$) (Student's t -test). (B) Morphology change of fat body cells after dsFoxO treatment versus dsGFP controls at 8 days post adult eclosion. Blue, nuclei; green, F-actin. Scale bars: 20 μ m. (C) Flow cytometry analysis showing the DNA content of fat body cells after dsFoxO treatment versus dsGFP controls at 8 days post adult eclosion. (D) The change of VgA and VgB mRNA and protein levels in the fat body of dsFoxO-treated adult females versus dsGFP controls at 8 days post adult eclosion. * $P < 0.05$ compared with the respective dsGFP controls ($n=8$) (Student's t -test). (E) Representative phenotypes of ovaries and primary oocytes subjected to dsFoxO treatment versus the dsGFP control at 8 days post adult eclosion. Ov, ovary; Ol, ovariole; Po, primary oocyte. Scale bars: black, 5 mm; white, 0.5 mm. (F) Statistical analysis for length \times width index of primary oocytes of dsFoxO- and dsGFP-treated adult females at 8 days post adult eclosion. *** $P < 0.001$ compared with the dsGFP control ($n=30$) (Student's t -test). The box plot comprises five values: the minimum, the 10th percentile, the median, the 90th percentile and the maximum values. The box indicates the 10th and 90th percentile values, while the whiskers indicate the 10th percentile values to the minimum or the 90th percentile values to the maximum.

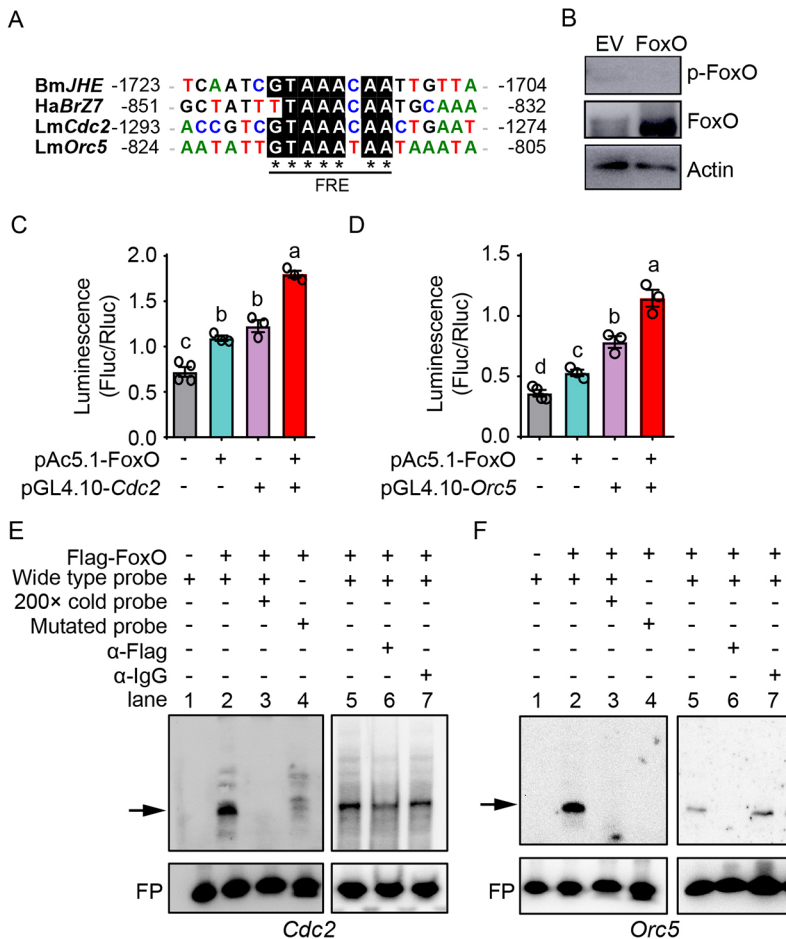


Fig. 6. Transcriptional upregulation of *Cdc2* and *Orc5* by FoxO. (A) Alignment of DNA sequences containing FoxO response element (FRE) in the promoters of *JHE* from *Bombyx mori* (Bm), *BrZ7* from *Helicoverpa armigera* (Ha), and *Cdc2* and *Orc5* from *L. migratoria* (Lm). (B) Western blots showing the expression of Flag-tagged FoxO and p-FoxO in S2 cells transfected with pAc5.1/Flag-FoxO compared with pAc5.1/Flag empty vector (EV). Anti-Flag and anti-p-FoxO were used to detect ectopic FoxO and P-FoxO, respectively. (C) Luciferase reporter assays using S2 cells transfected with pGL4.10 empty vector+pAc5.1/Flag empty vector, pGL4.10 empty vector+pAc5.1/Flag-FoxO, pGL4.10/Cdc2+pAc5.1/Flag empty vector and pGL4.10/Cdc2+pAc5.1/Flag-FoxO. Means labeled with different letters indicate significant difference at $P < 0.05$ ($n=3$) (Tukey's post-hoc test). (D) Luciferase reporter assays using S2 cells transfected with pGL4.10 empty vector+pAc5.1/Flag-FoxO, pGL4.10/Orc5+pAc5.1/Flag empty vector and pGL4.10/Orc5+pAc5.1/Flag-FoxO. Means labeled with different letters indicate significant difference at $P < 0.05$ ($n=3$) (Tukey's post-hoc test). (E,F) EMSA using the biotin-labeled *Cdc2* probe (E), biotin-labeled *Orc5* (F) probe, biotin-labeled mutated probe and non-labeled cold probe incubated with nuclear protein extracts from S2 cells with expressed Flag-FoxO anti-Flag antibody or a nonspecific antibody. The arrow indicates the specific band. FP, free probe.

with 8C and 16C peaks in the fat body of dsGFP controls, *Cdc2*-depleted fat bodies showed a 2C peak along with small populations of 8C and 16C (Fig. 7C). When *Orc5* was knocked down, fat body cells were chiefly 4C plus 2C and 8C populations (Fig. 7C). Knockdown of *Cdc2* caused 72.3% and 51% reductions of *VgA* and *VgB* transcripts, respectively (Fig. 7D). With respect to *Orc5*, its knockdown led to 57% and 87% reductions of *VgA* and *VgB* mRNA levels, respectively (Fig. 7D). The protein levels of *VgA* and *VgB* also markedly decreased in *Cdc2*- and *Orc5*-depleted fat bodies (Fig. 7D). As a result, both *Cdc2*- and *Orc5*-depleted adult females had severely impaired oocyte maturation and arrested ovarian growth (Fig. 7E), underscored by a dramatically lower length \times width index of the primary oocytes (Fig. 7F). Collectively, the above observations indicate a pivotal role for *Cdc2* and *Orc5* in fat body cell polyploidization, vitellogenesis and oocyte maturation.

DISCUSSION

Involvement of FoxO, *Cdc2* and *Orc5* in JH-stimulated polyploidization and vitellogenesis

JH plays a pivotal role in the onset and progression of polyploidy by promoting endocycle in locust fat body. During vitellogenesis, locust fat body nuclei undergo extensive DNA replication to produce highly polyploid cells, which can be blocked by allatectomy and restored by topical application of JH (Guo et al., 2014). This JH-dependent polyploidization in the adult female facilitates an accelerated synthesis of Vg that is essential for synchronous maturation of multiple eggs (Guo et al., 2014; Wu et al., 2016, 2018). In efforts to

identify genes involved in JH-dependent polyploidization, we initially performed RNA-seq analysis followed by qRT-PCR validation and found that 29 genes in DNA replication and cell cycle progression were upregulated by JH (Guo et al., 2014). Further studies revealed that JH acts through Met to regulate the transcription of two DNA replication genes, *Mcm4* and *Mcm7*, as well as three cell cycle genes, *Cdc6*, *Cdk6* and *E2f1* (Guo et al., 2014; Wu et al., 2016, 2018). In the present study, we demonstrated that RNAi-mediated knockdown of *FoxO*, *Cdc2* or *Orc5* in vitellogenic females resulted in lower ploidy and significantly reduced *Vg* expression in the fat body, as well as blocked oocyte maturation and arrested ovarian growth, similar to that caused by JH-deprivation or depletion of *Mcm4*, *Mcm7*, *Cdc6*, *Cdk6* and *E2f1* (Guo et al., 2014; Wu et al., 2016, 2018). Therefore, our current study provides the evidence that *FoxO*, *Cdc2* and *Orc5* are crucial players in JH-dependent polyploidization, vitellogenesis and egg development, which extends the view of JH action in insect cell polyploidization and vitellogenesis.

FoxO plays a crucial role in mediating the crosstalk between insulin and JH signaling to coordinate insect development and reproduction (Koyama et al., 2013; Roy et al., 2018; Santos et al., 2019; Smykal and Raikhel, 2015). In the cockroach *B. germanica*, *FoxO* RNAi in fed females caused substantially reduced *Vg* expression and arrested oocyte growth, without significant inhibition of JH synthesis (Abrisqueta et al., 2014). Similarly, *FoxO* knockdown caused reduction of *Vg* mRNA levels in fed adult females of the beetle *T. castaneum* (Parthasarathy and Palli, 2011).

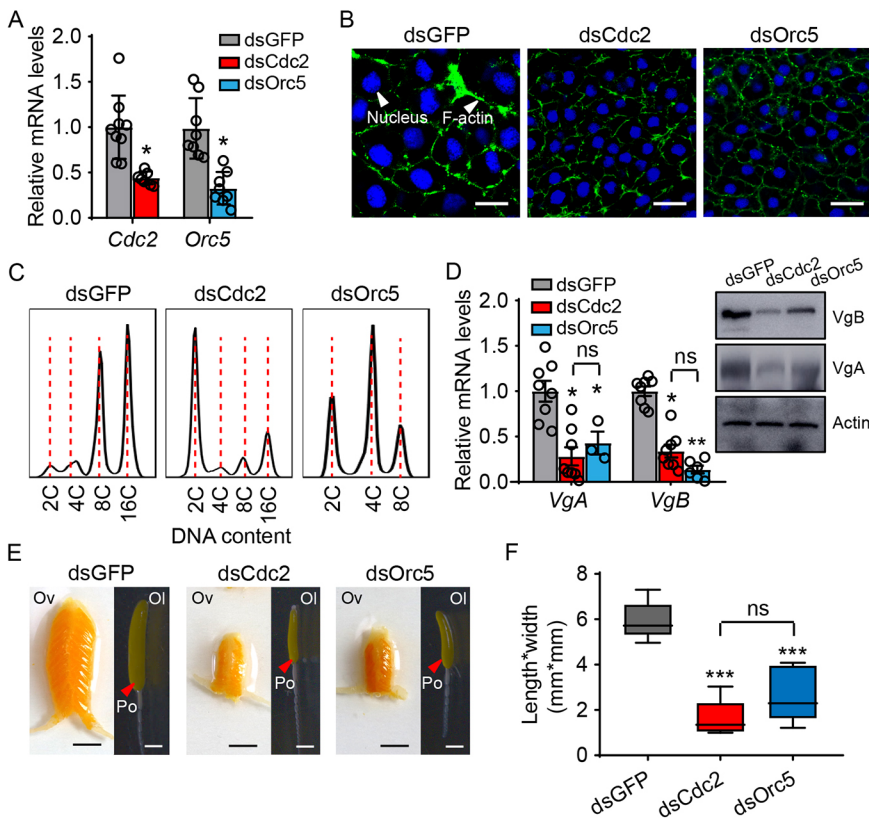


Fig. 7. Effect of *Cdc2* and *Orc5* RNAi on fat body cell ploidy and vitellogenesis. (A) Knockdown efficiency of *Cdc2* and *Orc5* RNAi in the fat body of adult females treated with ds*Cdc2* and ds*Orc5*, respectively. * $P < 0.05$ compared with the respective dsGFP controls ($n=8$) (Student's *t*-test). (B) Morphology change of fat body cells of adult females treated with ds*Cdc2* or ds*Orc5* versus dsGFP controls at 8 days post adult eclosion. Blue, nuclei; green, F-actin. Scale bars: 20 μ m. (C) Flow cytometry analysis showing the DNA content in the fat body cells of adult females treated with ds*Cdc2* or ds*Orc5* versus dsGFP controls at 8 days post adult eclosion. Scale bars: black, 5 mm; white, 0.5 mm. (D) qRT-PCR and western blot showing mRNA and protein levels of VgA and VgB in the fat body of ds*Cdc2*- and ds*Orc5*-treated adult females at 8 days post adult eclosion. * $P < 0.05$ and ** $P < 0.01$ compared with dsGFP controls. ns, no significant difference ($n=8$) (Student's *t*-test). (E) Representative phenotypes of ovaries and primary oocytes subjected to ds*Cdc2* or ds*Orc5* versus dsGFP controls at 8 days post adult eclosion. Ov, ovary; Ol, ovariole; Po, primary oocyte. Scale bars: black, 5 mm; white, 0.5 mm. (F) Statistical analysis for length \times width index of primary oocytes of ds*Cdc2*-, ds*Orc5*- and dsGFP-treated adult females at 8 days post adult eclosion. *** $P < 0.001$ compared with the dsGFP control. ns, no significant difference ($n=30$) (Student's *t*-test). The box plot comprises five values: the minimum, the 10th percentile, the median, the 90th percentile and the maximum values. The box indicates the 10th and 90th percentile values, while the whiskers indicate the 10th percentile values to the minimum or the 90th percentile values to the maximum.

In the mosquito *Ae. aegypti*, *FoxO* knockdown repressed *Vg* expression, resulting in a low rate of reproduction (Hansen et al., 2007). Depletion of *FoxO* also suppressed *Vg* expression and reduced ovarian development in the soybean pod borer *Maruca vitrata* (Al Baki et al., 2019). These studies together support our observation that *FoxO* knockdown in vitellogenic female locusts led to significantly reduced *Vg* expression along with blocked oocyte maturation and arrested ovarian growth. Conversely, the inhibitory roles of *FoxO* in reproduction have been reported in insects under starvation or poor nutrients. For example, in contrast to fed females, *FoxO* RNAi in starved cockroach females elicited an increase of JH biosynthesis, concomitant with remarkable increase of *Vg* expression and accelerated growth of oocytes (Abrisqueta et al., 2014; Sren-Castillo et al., 2012). In the diapausing mosquito *Culex pipiens*, insulin pathway shut down leads to activated *FoxO* and arrested ovarian development (Sim and Denlinger, 2013). Application of JH to diapause-destined females suppressed *FoxO* activity and then restored ovarian development (Sim and Denlinger, 2013). Our data, together with the above reports, suggest that *FoxO* has dual functions in the reproduction of diverse insect species, depending on nutrients and gonadotrophins.

Interestingly, *FoxO* knockdown led to considerably reduced ploidy, as determined by confocal imaging and quantitative analysis with flow cytometry. This is opposite to the situation found in *D. melanogaster* starved adult females. The mitotic-to-endocycle (M/E) transition is a crucial step during fruit fly oogenesis (Gruntenko and Rauschenbach, 2018). In the absence of nutritional stress, *FoxO* was dispensable for the M/E switch. However, upon starvation, *FoxO* was essential for triggering the paused M/E switch, blocking the entry of egg chambers into vitellogenesis (Jouandin et al., 2014). In contrast to starved fruit flies, locusts in the present study were normally fed, which might partially explain the opposite results from these two studies. It also suggests the involvement of

other factors, as JH governs ploidy-dependent vitellogenesis and oogenesis of locusts, whereas 20E regulates follicle cell polyploidization and oogenesis in *D. melanogaster*. Like *FoxO* knockdown, depletion of *Cdc2* or *Orc5* resulted in significantly lower ploidy in fat body cells, along with reduced *Vg* expression, blocked oocyte maturation and arrested ovarian growth. Interestingly, the defective phenotypes caused by *Cdc2* knockdown were more severe than those cause by *Orc5* knockdown. The results suggest that *Cdc2* might be more potent than *Orc5* in mediating the progression of endocycle and polyploidization. *Cdc2* is a crucial player in the regulation of cell cycle, not only promoting G2-M transition but also driving G1 progression and G1-S transition (Enserink and Kolodner, 2010; Woodbury and Morgan, 2007). *Orc5* is a key component of the prereplication complex at G1 phase and is essential for initiation of DNA replication at S phase (Lei and Tye, 2001; Riera and Speck, 2015; Takara and Bell, 2011).

JH-LCMT1-PP2A signaling cascade and *FoxO* dephosphorylation

We observed that p-*FoxO* levels elevated during the previtellogenic stage but then markedly dropped in the vitellogenic phase, whereas *FoxO* was constantly expressed at both mRNA and protein levels. The reduction of p-*FoxO* abundance during vitellogenic stage suggests a link between *FoxO* dephosphorylation and the high level or a peak of JH titers in this duration. When JH-deprived fat bodies were further treated with methoprene, p-*FoxO* abundance increased at 6 h but then declined post 12 h, indicating that longer treatment of JH stimulates *FoxO* dephosphorylation. Intriguingly, Akt, p-Akt and p-PP2A abundance had no apparent change during the first gonadotrophic cycle. In contrast, m-PP2A abundance and PP2A activity in the fat body substantially increased on day 4 and remained high thereafter. Moreover, deprivation of endogenous JH inhibited PP2A methylation and activity, and additional application

of methoprene led to obvious increase of PP2A methylation and activity. A similar pattern was seen with the methyltransferase LCMT1. We therefore raised the hypothesis that FoxO dephosphorylation was mediated by JH-stimulated and LCMT1-dependent PP2A methylation. Indeed, when *LCMT1* was depleted, m-PP2A abundance and PP2A activity markedly reduced, and p-FoxO levels showed concomitant increase. Previously, LCMT1-triggered PP2A methylation (Sents et al., 2013; Sontag et al., 2013) and PP2A-mediated FoxO dephosphorylation (Singh et al., 2010; Yadav et al., 2017) have been reported in vertebrates. However, the regulation of LCMT1 methyltransferase activity has not been elucidated, except for a study describing the potential involvement of GSK-3 β in the regulation of LCMT1 activity (Wang et al., 2015). As *Met* RNAi had no effect on *LCMT1* expression, it is conceivable that JH might act through a membrane signaling cascade to stimulate LCMT1 activity. It must be noted that the JH-deprived condition was achieved by precocene treatment on newly emerged adult females for 10 days, which covered the first gonadotrophic cycle. No apparent increase of p-FoxO was observed in precocene-treated adult females compared with 10-day-old individuals. However, precocene treatment caused reduced levels of LCMT1 expression and PP2A methylation, and *LCMT1* or *PP2A* knockdown led to increased levels of p-FoxO. These observations suggest the possible involvement of other factors beyond JH-LCMT1-PP2A axis in regulating FoxO dephosphorylation.

PP2A-mediated FoxO dephosphorylation facilitates its translocation in nuclei and transcriptional activity (Singh et al., 2010; Yadav et al., 2017). Interestingly, *Cdc2* and *Orc5* were expressed in response to JH and FoxO, and their upstream sequences possess the conserved FRE motif found in the upstream of other FoxO-targeting genes like *4eBP*, β -*catenin* and *hid* (Cai et al., 2016; Luo et al., 2007; Mahoney et al., 2016; Zeng et al., 2017; Zhang et al., 2016). Our EMSA and dual luciferase assays further documented that FoxO bound to their FRE-containing sequences and activated the transcription of *Cdc2* and *Orc5*. The induction of target gene transcription by FoxO have been previously reported. In *H. armigera*, increased titers of 20E promoted FoxO expression and repressed FoxO phosphorylation. FoxO in nuclei then bound to FRE in the promoter of *BrZ7* gene to induce its expression (Cai et al., 2016). In the silkworm *Bombyx mori*, FoxO bound to FRE in the promoters of *brummer* and *acid lipase-1*, consequently inducing their expression for fat body lipolysis (Hossain et al., 2013). Nevertheless, the inhibitory effect of FoxO on target gene transcription has also been reported. In *T. castaneum*, FoxO bound to *Vg2* gene promoter and inhibited its transcription (Sheng et al., 2011). After adult beetle emergence, JH induced *ILP* expression and stimulated FoxO phosphorylation, which in turn released FoxO binding and activated *Vg2* transcription (Sheng et al., 2011). In *B. mori*, FoxO was involved in the repression of JH degradation genes *JHE*, *JHDK* and *JHEH*. FoxO mutation eliminated this suppression effect, resulting in activation of these genes to accelerate JH degradation (Zeng et al., 2017). Future discoveries of new players that modulate FoxO function should explain how FoxO exerts its dual functions in regulating target gene transcription. A recent study reported that Kr-h1, a key player in JH pathway, bound to FoxO and inhibited the expression of *InR* and *brummer* by influencing the binding affinity of FoxO to its DNA element (Kang et al., 2017).

In summary, this study provides an evidence that JH acts through LCMT1-PP2A-FoxO-Cdc2/Orc5 to promote fat body cell polyploidization and vitellogenesis. The results thus fill the gap in our knowledge about the regulatory mechanisms of JH-stimulated

polyploidization and vitellogenesis beyond the JH-Met-endocycle genes axis. Although we could not exclude the involvement of other potential signaling molecules, the findings in our present study, together with our previous reports, suggest that JH stimulates the expression of *Cdc2* and *Orc5* through LCMT1-PP2A-FoxO while inducing the expression of *Mcm4/7*, *Cdc6*, *Cdk6* and *E2f1* via *Met*/Tai. These two signaling pathways cooperate to promote fat body cell polyploidization for accelerated synthesis of Vg, consequently meeting the requirement of synchronous maturation of multiple eggs.

MATERIALS AND METHODS

Experimental animals

Locusts were maintained in gregarious phase under a photoperiod of 14L:10D and at 30 \pm 2°C. The diet included a continuous supply of wheat bran with fresh wheat seedlings provided once daily. JH-deprived female adult locusts were obtained by inactivation of the corpora allata via topical application of 500 μ g (100 μ g/ μ l dissolved in acetone) precocene III (Sigma-Aldrich) within 12 h PAE. JH activity was restored by topical administration of s-(+)-methoprene (Santa Cruz Biotech) at 150 μ g (30 μ g/ μ l dissolved in acetone) per locust 10 days post precocene treatment. For inhibition of PP2A activity, okadaic acid (Sigma-Aldrich) at 0.2 mM was applied to adult females at 3 days PAE.

RNA extraction and qRT-PCR

Total RNA was extracted from fat bodies using Trizol reagent (Tiangen) as previous reported (Wang et al., 2017; Wu et al., 2018; Zheng et al., 2020). cDNA was reverse-transcribed using FastQuant RT Kit with gDNase (Tiangen). qRT-PCR was performed using SYBR Green SuperReal PreMix (Tiangen) and a LightCycler 96 system (Roche), initiated at 95°C for 2 min, followed by 40 cycles of 95°C for 20 s, 58°C for 20 s and 72°C for 30 s. The relative expression levels were calculated using the $2^{-\Delta\Delta C_t}$ method, with ribosomal protein 49 (rp49) as the reference control. Melting curve analysis was conducted to verify the specificity of amplification. Primers used in qRT-PCR are listed in Table S1.

RNA interference, tissue imaging and confocal microscopy

Double-stranded RNA was synthesized by *in vitro* transcription using T7 RiboMAX Express RNAi system (Promega). Adult females within 12 h after adult eclosion were intra-abdominally injected with 15 μ g (5 μ g/ μ l) dsRNA and boosted at 5 days PAE, and phenotypes were examined at 8 days PAE. Injection of green fluorescent protein (GFP) dsRNA was used as the mock control. Primers used for synthesis of dsRNA are included in Table S1. Ovaries and ovarioles were photographed using a Canon EOS550D camera and Leica M205C stereomicroscope, respectively. The size of the primary oocytes was measured with Image-Pro Plus 6.0 software. For cell staining, fat bodies were fixed in 4% paraformaldehyde and permeabilized in 0.3% Triton X-100. F-actin and nuclei were stained with 0.165 μ M Phalloidin-Alexa Fluor 488 (Invitrogen) and 5 μ M Hoechst 33342 (Sigma-Aldrich), respectively. Cell images were captured with a Zeiss LSM 710 confocal microscope and processed with ZEN2012 software (Carl Zeiss).

Flow cytometry

Fat body cells were collected by centrifugation (800 g) of homogenized tissues, fixed in 70% ethanol overnight and further incubated for 2 h at 4°C with PBS buffer containing 100 μ g/ml RNaseA (Promega), 50 μ g/ml propidium iodide (Sigma-Aldrich) and 0.2% Triton X-100. After filtration with a 300-mesh cell strainer (BD Falcon), the cells were analyzed using a BD FACSCalibur Flow Cytometry System and Flowjo 7.6.1 software (BD Biosciences). A total of 40 mg of fat bodies was used in each experiment, and six independent experiments were carried out for each treatment. Locust brain nuclei were used as the diploid reference standard.

Antiserum preparation

cDNA fragments of locust FoxO (GenBank: MN427928) and LCMT1 (GenBank: MN427929) were amplified with the specific primers

(Table S1), cloned into pET-32a(+)-His and confirmed by sequencing. The recombinant proteins were expressed in Rosetta host cells under Isopropyl- β -D-thiogalactopyranoside induction, purified using a Ni²⁺-NTA affinity column (CWbiotech) and examined by SDS-PAGE. Polyclonal antisera were raised in New Zealand White rabbits using the purified proteins mixed with Freund's complete adjuvant (Sigma-Aldrich) to form a stable emulsion for immunization. The rabbits were injected subcutaneously at four sites and boosted once a week either four or five times. The antiserum specificity was verified from fat bodies of adult females subjected to respective gene knockdown. The antisera of locust Vg and β -actin were raised as previously described (Jing et al., 2018; Luo et al., 2017).

Protein extraction and western blot

The locust *FoxO*-coding region (amino acid 1-486) was cloned into pAc5.1/Flag vector (Invitrogen) to obtain a Flag-FoxO fusion protein in *Drosophila* S2 cells (cells were kindly provided by the Stem Cell Bank, Chinese Academy of Science). S2 cells were transfected with pAc5.1/Flag-FoxO using Lipofectamine 3000 (Invitrogen) for 48 h. Total protein extracts from locust fat bodies or S2 cells were collected using the ice-cold lysis buffer containing 50 mM Tris-HCl (pH 7.5), 150 mM NaCl, 2 mM EDTA, 1 mM DTT, 1% Nonidet P-40, 1 mM NaF and 1 mM PMSF, plus the protease and phosphatase inhibitor cocktails (Roche). Lysates were cleared by centrifugation at 14,000 \times g at 4°C for 10 min, fractionated on 8% SDS-PAGE and transferred to PVDF membranes (Millipore). Western blots were conducted using the specific antibodies against FoxO, p-FoxO (Abcam, ab131339), PP2A (Cell Signaling Technology, 2038T), p-PP2A (R&D Systems, YZW0418081), m-PP2A (Abcam, ab66597), Akt (Cell Signaling Technology, 9272S), p-Akt (Cell Signaling Technology, 4060S), LCMT1, Vg and Flag (MBL, M185-3S), the corresponding HRP-conjugated secondary antibodies (CWbiotech), and an enhanced chemiluminescent reagent (Boster). Locust β -actin antibody was used as the loading control. Bands were imaged using an Amersham Imager 600 (GE Healthcare).

Luciferase reporter assay

The promoters of *Cdc2* (GenBank: MN480458) and *Orc5* (GenBank: MN480459) were amplified by PCR, separately cloned into a pGL4.10 vector (Promega), and confirmed by sequencing. The recombinant vectors pGL4.10-*Cdc2*^{-1912 to -1041} and pGL4.10-*Orc5*^{-1115 to -46} or pGL4.10 empty vector were separately transfected into S2 cells with either pAc5.1/Flag empty vector or pAc5.1/Flag-FoxO using Lipofectamine 3000 (Invitrogen). After 48 h, luciferase activity was then measured using a Dual-luciferase Reporter Assay System and a GloMax 96 Microplate Luminometer (Promega).

Electrophoretic mobility shift assay (EMSA)

Nuclear extracts from S2 cells were isolated using NE-PER Nuclear and Cytoplasmic Extraction Reagents kit (Thermo Fisher Scientific). The *Cdc2* probe (ACCGTCGTAACAACACTGAAT) and *Orc5* probe (AATATTGTAATAATAAATA) were end-labeled with biotin, and incubated with nuclear protein extracts using the LightShift Chemiluminescent EMSA Kit (Thermo Fisher Scientific). In the competition assays, a 200 \times molar excess of unlabeled *Cdc2* or *Orc5* probe was added into the binding reaction. In the supershift assays, anti-Flag antibody (MBL) or the control IgG (Sigma-Aldrich) was pre-incubated with the nuclear extracts for 1 h at 4°C prior to the addition of labeled probes. The DNA-protein complex was resolved in 5% native polyacrylamide gels and visualized using an Amersham Imager 600 (GE healthcare).

PP2A activity assay

ELISA was conducted to measure PP2A activity using a Serine/Threonine Phosphatase assay System (Promega) following the manufacturer's instruction. Briefly, samples were lysed in the ice-cold lysis buffer containing 50 mM Tris-HCl (pH 7.5), 150 mM NaCl, 2 mM EDTA, 1 mM DTT, 1% Nonidet P-40, 1 mM NaF and 1 mM PMSF. The endogenous phosphate was removed by centrifugation with supplied spin columns. The extracts were then normalized for protein content and incubated with substrate (chemically synthesized phosphopeptide RRA(pT)VA). Subsequently, 50 μ l Molybdate Dye/Additive mixture was added and further incubated for 30 min at room temperature. The

absorbance of molybdate-malachite green-phosphate was measured with a spectrophotometer (Molecular Devices) at 630 nm.

Data analysis

Statistical analyses were performed with Student's *t*-test or one-way analysis of variance (ANOVA) with Tukey's post-hoc test using the SPSS20.0 software. Significant difference was considered at $P < 0.05$. Values are represented by mean \pm s.e.m.

Competing interests

The authors declare no competing or financial interests.

Author contributions

Conceptualization: Z.W., S.Z.; Methodology: Z.W., Q.H., S.Z.; Software: Z.W., Q.H., H.Z., S.Z.; Validation: Z.W., S.Z.; Formal analysis: Z.W., S.Z.; Investigation: Z.W., Q.H., H.Z., S.Z.; Resources: Z.W., S.Z.; Data curation: Z.W., Q.H., B.Z., H.Z., S.Z.; Writing - original draft: Z.W., S.Z.; Writing - review & editing: Z.W., S.Z.; Visualization: Z.W., Q.H., S.Z.; Supervision: Z.W., S.Z.; Project administration: Z.W., S.Z.; Funding acquisition: S.Z.

Funding

This work was supported by National Natural Science Foundation of China (NSFC) grant U1804232. Deposited in PMC for immediate release.

Supplementary information

Supplementary information available online at <https://dev.biologists.org/lookup/doi/10.1242/dev.188813.supplemental>

Peer review history

The peer review history is available online at <https://dev.biologists.org/lookup/doi/10.1242/dev.188813.reviewer-comments.pdf>

References

- Abriskueta, M., Süren-Castillo, S. and Maestro, J. L. (2014). Insulin receptor-mediated nutritional signalling regulates juvenile hormone biosynthesis and vitellogenin production in the German cockroach. *Insect Biochem. Mol. Biol.* **49**, 14-23. doi:10.1016/j.ibmb.2014.03.005
- Al Baki, M. A., Lee, D. W., Jung, J. K. and Kim, Y. (2019). Insulin signaling mediates previtellogenic development and enhances juvenile hormone-mediated vitellogenesis in a lepidopteran insect, *Maruca vitrata*. *BMC Dev. Biol.* **19**, 14. doi:10.1186/s12861-019-0194-8
- Belles, X. (2004). Vitellogenesis directed by juvenile hormone. In *Reproductive Biology of Invertebrates* (ed. A. S. Raikhel), pp. 157-197. Enfield/Plymouth: Science Publisher, Inc.
- Buntrock, L., Marec, F., Krueger, S. and Traut, W. (2012). Organ growth without cell division: somatic polyploidy in a moth, *Ephesia kuehniella*. *Genome* **55**, 755-763. doi:10.1139/g2012-060
- Cai, M.-J., Liu, W., Pei, X.-Y., Li, X.-R., He, H.-J., Wang, J.-X. and Zhao, X.-F. (2014). Juvenile hormone prevents 20-hydroxyecdysone-induced metamorphosis by regulating the phosphorylation of a newly identified broad protein. *J. Biol. Chem.* **289**, 26630-26641. doi:10.1074/jbc.M114.581876
- Cai, M.-J., Zhao, W.-L., Jing, Y.-P., Song, Q., Zhang, X.-Q., Wang, J.-X. and Zhao, X.-F. (2016). 20-hydroxyecdysone activates Forkhead box O to promote proteolysis during *Helicoverpa armigera* molting. *Development* **143**, 1005-1015. doi:10.1242/dev.128694
- Charles, J.-P., Iwema, T., Epa, V. C., Takaki, K., Rynes, J. and Jindra, M. (2011). Ligand-binding properties of a juvenile hormone receptor, Methoprene-tolerant. *Proc. Natl. Acad. Sci. USA* **108**, 21128-21133. doi:10.1073/pnas.1116123109
- Edgar, B. A. and Orr-Weaver, T. L. (2001). Endoreplication cell cycles: more for less. *Cell* **105**, 297-306. doi:10.1016/S0092-8674(01)00334-8
- Edgar, B. A., Zielke, N. and Gutierrez, C. (2014). Endocycles: a recurrent evolutionary innovation for post-mitotic cell growth. *Nat. Rev. Mol. Cell Biol.* **15**, 197-210. doi:10.1038/nrm3756
- Enserink, J. M. and Kolodner, R. D. (2010). An overview of Cdk1-controlled targets and processes. *Cell Div.* **5**, 11. doi:10.1186/1747-1028-5-11
- Gruntenko, N. E. and Rauschenbach, I. Y. (2018). The role of insulin signalling in the endocrine stress response in *Drosophila melanogaster*. A mini-review. *Gen. Comp. Endocrinol.* **258**, 134-139. doi:10.1016/j.ygcen.2017.05.019
- Guo, W., Wu, Z., Song, J., Jiang, F., Wang, Z., Deng, S., Walker, V. K. and Zhou, S. (2014). Juvenile hormone-receptor complex acts on *mcm4* and *mcm7* to promote polyploidy and vitellogenesis in the migratory locust. *PLoS Genet.* **10**, e1004702. doi:10.1371/journal.pgen.1004702
- Guo, W., Wu, Z., Yang, L., Cai, Z., Zhao, L. and Zhou, S. (2019). Juvenile hormone-dependent Kazal-type serine protease inhibitor Greglin safeguards

- insect vitellogenesis and egg production. *FASEB J.* **33**, 917-927. doi:10.1096/fj.201801068R
- Hansen, I. A., Sieglaff, D. H., Munro, J. B., Shiao, S.-H., Cruz, J., Lee, I. W., Heraty, J. M. and Raikhel, A. S.** (2007). Forkhead transcription factors regulate mosquito reproduction. *Insect Biochem. Mol. Biol.* **37**, 985-997. doi:10.1016/j.ibmb.2007.05.008
- Hossain, M. S., Liu, Y., Zhou, S., Li, K., Tian, L. and Li, S.** (2013). 20-Hydroxyecdysone-induced transcriptional activity of FoxO upregulates *brummer* and *acid lipase-1* and promotes lipolysis in *Bombyx* fat body. *Insect Biochem. Mol. Biol.* **43**, 829-838. doi:10.1016/j.ibmb.2013.06.007
- Jacobson, A. L., Johnston, J. S., Rotenberg, D., Whitfield, A. E., Booth, W., Vargo, E. L. and Kennedy, G. G.** (2013). Genome size and ploidy of Thysanoptera. *Insect Mol. Biol.* **22**, 12-17. doi:10.1111/j.1365-2583.2012.01165.x
- Janssens, V. and Goris, J.** (2001). Protein phosphatase 2A: a highly regulated family of serine/threonine phosphatases implicated in cell growth and signalling. *Biochem. J.* **353**, 417-439. doi:10.1042/bj3530417
- Janssens, V., Longin, S. and Goris, J.** (2008). PP2A holoenzyme assembly: in cauda venenum (the sting is in the tail). *Trends Biochem. Sci.* **33**, 113-121. doi:10.1016/j.tibs.2007.12.004
- Jindra, M., Bellés, X. and Shinoda, T.** (2015). Molecular basis of juvenile hormone signaling. *Curr. Opin. Insect Sci.* **11**, 39-46. doi:10.1016/j.cois.2015.08.004
- Jindra, M., Palli, S. R. and Riddiford, L. M.** (2013). The juvenile hormone signaling pathway in insect development. *Annu. Rev. Entomol.* **58**, 181-204. doi:10.1146/annurev-ento-120811-153700
- Jing, Y.-P., An, H., Zhang, S., Wang, N. and Zhou, S.** (2018). Protein kinase C mediates juvenile hormone-dependent phosphorylation of Na(+)/K(+)-ATPase to induce ovarian follicular patency for yolk protein uptake. *J. Biol. Chem.* **293**, 20112-20122. doi:10.1074/jbc.RA118.005692
- Jouandin, P., Ghigliione, C. and Noselli, S.** (2014). Starvation induces FoxO-dependent mitotic-to-endocycle switch pausing during *Drosophila* oogenesis. *Development* **141**, 3013-3021. doi:10.1242/dev.108399
- Kang, P., Chang, K., Liu, Y., Bouska, M., Birnbaum, A., Karashchuk, G., Thakore, R., Zheng, W., Post, S., Brent, C. S. et al.** (2017). *Drosophila* Kruppel homolog 1 represses lipolysis through interaction with dFOXO. *Sci. Rep.* **7**, 16369. doi:10.1038/s41598-017-16638-1
- Kayukawa, T., Minakuchi, C., Namiki, T., Togawa, T., Yoshiyama, M., Kamimura, M., Mita, K., Imanishi, S., Kiuchi, M., Ishikawa, Y. et al.** (2012). Transcriptional regulation of juvenile hormone-mediated induction of *Kruppel homolog 1*, a repressor of insect metamorphosis. *Proc. Natl. Acad. Sci. USA* **109**, 11729-11734. doi:10.1073/pnas.1204951109
- Koyama, T., Iwami, M. and Sakurai, S.** (2004). Ecdysteroid control of cell cycle and cellular commitment in insect wing imaginal discs. *Mol. Cell. Endocrinol.* **213**, 155-166. doi:10.1016/j.mce.2003.10.063
- Koyama, T., Mendes, C. C. and Mirth, C. K.** (2013). Mechanisms regulating nutrition-dependent developmental plasticity through organ-specific effects in insects. *Front. Physiol.* **4**, 263. doi:10.3389/fphys.2013.00263
- Lei, M. and Tye, B. K.** (2001). Initiating DNA synthesis: from recruiting to activating the MCM complex. *J. Cell Sci.* **114**, 1447-1454.
- Li, T.-R. and White, K. P.** (2003). Tissue-specific gene expression and ecdysone-regulated genomic networks in *Drosophila*. *Dev. Cell* **5**, 59-72. doi:10.1016/S1534-5807(03)00192-8
- Li, M., Mead, E. A. and Zhu, J.** (2011). Heterodimer of two bHLH-PAS proteins mediates juvenile hormone-induced gene expression. *Proc. Natl. Acad. Sci. USA* **108**, 638-643. doi:10.1073/pnas.1013914108
- Li, K., Jia, Q. Q. and Li, S.** (2019). Juvenile hormone signaling - a mini review. *Insect Sci.* **26**, 600-606. doi:10.1111/1744-7917.12614
- Liu, P., Peng, H.-J. and Zhu, J.** (2015). Juvenile hormone-activated phospholipase C pathway enhances transcriptional activation by the methoprene-tolerant protein. *Proc. Natl. Acad. Sci. USA* **112**, E1871-E1879. doi:10.1073/pnas.1423204112
- Liu, P., Fu, X. and Zhu, J.** (2018). Juvenile hormone-regulated alternative splicing of the *taiman* gene primes the ecdysteroid response in adult mosquitoes. *Proc. Natl. Acad. Sci. USA* **115**, E7738-E7747. doi:10.1073/pnas.1808146115
- Luo, X., Puig, O., Hyun, J., Bohmann, D. and Jasper, H.** (2007). Foxo and Fos regulate the decision between cell death and survival in response to UV irradiation. *EMBO J.* **26**, 380-390. doi:10.1038/sj.emboj.7601484
- Luo, M., Li, D., Wang, Z., Guo, W., Kang, L. and Zhou, S.** (2017). Juvenile hormone differentially regulates two *Gpr78* genes encoding protein chaperones required for insect fat body cell homeostasis and vitellogenesis. *J. Biol. Chem.* **292**, 8823-8834. doi:10.1074/jbc.M117.780957
- Mahoney, R. E., Azpurua, J. and Eaton, B. A.** (2016). Insulin signaling controls neurotransmission via the 4eBP-dependent modification of the exocytotic machinery. *Elife* **5**, e16807. doi:10.7554/eLife.16807.016
- Manning, B. D. and Toker, A.** (2017). AKT/PKB Signaling: Navigating the Network. *Cell* **169**, 381-405. doi:10.1016/j.cell.2017.04.001
- Mirth, C. K., Tang, H. Y., Makohon-Moore, S. C., Salhadar, S., Gokhale, R. H., Warner, R. D., Koyama, T., Riddiford, L. M. and Shingleton, A. W.** (2014). Juvenile hormone regulates body size and perturbs insulin signaling in *Drosophila*. *Proc. Natl. Acad. Sci. USA* **111**, 7018-7023. doi:10.1073/pnas.1313058111
- Moriyama, M., Osanai, K., Ohyoshi, T., Wang, H.-B., Iwanaga, M. and Kawasaki, H.** (2016). Ecdysteroid promotes cell cycle progression in the *Bombyx* wing disc through activation of c-Myc. *Insect Biochem. Mol. Biol.* **70**, 1-9. doi:10.1016/j.ibmb.2015.11.008
- Nordman, J. and Orr-Weaver, T. L.** (2012). Regulation of DNA replication during development. *Development* **139**, 455-464. doi:10.1242/dev.061838
- Ohhara, Y., Kobayashi, S. and Yamanaka, N.** (2017). Nutrient-dependent endocycling in steroidogenic tissue dictates timing of metamorphosis in *Drosophila melanogaster*. *PLoS Genet.* **13**, e1006583. doi:10.1371/journal.pgen.1006583
- Ojani, R., Liu, P., Fu, X. and Zhu, J.** (2016). Protein kinase C modulates transcriptional activation by the juvenile hormone receptor methoprene-tolerant. *Insect Biochem. Mol. Biol.* **70**, 44-52. doi:10.1016/j.ibmb.2015.12.001
- Orr-Weaver, T. L.** (2015). When bigger is better: the role of polyploidy in organogenesis. *Trends Genet.* **31**, 307-315. doi:10.1016/j.tig.2015.03.011
- Parthasarathy, R. and Palli, S. R.** (2011). Molecular analysis of nutritional and hormonal regulation of female reproduction in the red flour beetle, *Tribolium castaneum*. *Insect Biochem. Mol. Biol.* **41**, 294-305. doi:10.1016/j.ibmb.2011.01.006
- Raikhel, A. S., Brown, M. R. and Belles, X.** (2005). Hormonal control of reproductive processes. In *Comprehensive Molecular Insect Science* (ed. L. I. Gilbert, K. Iatrou and S. S. Gill), pp. 433-491. Boston: Elsevier.
- Riddiford, L. M.** (1994). Cellular and molecular actions of juvenile hormone I. General considerations and premetamorphic actions. *Adv. In. Insect Phys.* **24**, 213-274. doi:10.1016/S0065-2806(08)60084-3
- Riera, A. and Speck, C.** (2015). Opening the gate to DNA replication. *Cell Cycle* **14**, 6-8. doi:10.4161/15384101.2014.987624
- Roy, S., Saha, T. T., Zou, Z. and Raikhel, A. S.** (2018). Regulatory pathways controlling female insect reproduction. *Annu. Rev. Entomol.* **63**, 489-511. doi:10.1146/annurev-ento-020117-043258
- Santos, C. G., Humann, F. C. and Hartfelder, K.** (2019). Juvenile hormone signaling in insect oogenesis. *Curr. Opin. Insect Sci.* **31**, 43-48. doi:10.1016/j.cois.2018.07.010
- Sents, W., Ivanova, E., Lambrecht, C., Haesen, D. and Janssens, V.** (2013). The biogenesis of active protein phosphatase 2A holoenzymes: a tightly regulated process creating phosphatase specificity. *FEBS J.* **280**, 644-661. doi:10.1111/j.1742-4658.2012.08579.x
- Sheng, Z., Xu, J., Bai, H., Zhu, F. and Palli, S. R.** (2011). Juvenile hormone regulates vitellogenin gene expression through insulin-like peptide signaling pathway in the red flour beetle, *Tribolium castaneum*. *J. Biol. Chem.* **286**, 41924-41936. doi:10.1074/jbc.M111.269845
- Sim, C. and Denlinger, D. L.** (2013). Juvenile hormone III suppresses forkhead of transcription factor in the fat body and reduces fat accumulation in the diapausing mosquito, *Culex pipiens*. *Insect Mol. Biol.* **22**, 1-11. doi:10.1111/j.1365-2583.2012.01166.x
- Singh, A., Ye, M., Bucur, O., Zhu, S., Tanya Santos, M., Rabinovitz, I., Wei, W., Gao, D., Yeh, W. C. and Khosravi-Far, R.** (2010). Protein phosphatase 2A reactivates FOXO3a through a dynamic interplay with 14-3-3 and AKT. *Mol. Biol. Cell* **21**, 1140-1152. doi:10.1091/mbc.e09-09-0795
- Smykal, V. and Raikhel, A. S.** (2015). Nutritional control of insect reproduction. *Curr. Opin. Insect Sci.* **11**, 31-38. doi:10.1016/j.cois.2015.08.003
- Song, J., Guo, W., Jiang, F., Kang, L. and Zhou, S.** (2013). Argonaute 1 is indispensable for juvenile hormone mediated oogenesis in the migratory locust, *Locusta migratoria*. *Insect Biochem. Mol. Biol.* **43**, 879-887. doi:10.1016/j.ibmb.2013.06.004
- Song, J., Li, W., Zhao, H. and Zhou, S.** (2019). Clustered miR-2, miR-13a, miR-13b and miR-71 coordinately target *Notch* gene to regulate oogenesis of the migratory locust *Locusta migratoria*. *Insect Biochem. Mol. Biol.* **106**, 39-46. doi:10.1016/j.ibmb.2018.11.004
- Sontag, J.-M., Nunbhakdi-Craig, V. and Sontag, E.** (2013). Leucine carboxyl methyltransferase 1 (LCMT1)-dependent methylation regulates the association of protein phosphatase 2A and tau protein with plasma membrane microdomains in neuroblastoma cells. *J. Biol. Chem.* **288**, 27396-27405. doi:10.1074/jbc.M113.490102
- Sun, J., Smith, L., Armento, A. and Deng, W.-M.** (2008). Regulation of the endocycle/genome amplification switch by Notch and ecdysone signaling. *J. Cell Biol.* **182**, 885-896. doi:10.1083/jcb.200802084
- Süren-Castillo, S., Abrisqueta, M. and Maestro, J. L.** (2012). FoxO inhibits juvenile hormone biosynthesis and vitellogenin production in the German cockroach. *Insect Biochem. Mol. Biol.* **42**, 491-498. doi:10.1016/j.ibmb.2012.03.006
- Takara, T. J. and Bell, S. P.** (2011). Multiple Cdt1 molecules act at each origin to load replication-competent Mcm2-7 helicases. *EMBO J.* **30**, 4885-4896. doi:10.1038/emboj.2011.394
- Wang, Y., Yang, R., Gu, J., Yin, X., Jin, N., Xie, S., Wang, Y., Chang, H., Qian, W., Shi, J. et al.** (2015). Cross talk between PI3K-AKT-GSK-3 β and PP2A pathways determines tau hyperphosphorylation. *Neurobiol. Aging* **36**, 188-200. doi:10.1016/j.neurobiolaging.2014.07.035
- Wang, Z., Yang, L., Song, J., Kang, L. and Zhou, S.** (2017). An isoform of Taiman that contains a PRD-repeat motif is indispensable for transducing the vitellogenetic

- juvenile hormone signal in *Locusta migratoria*. *Insect Biochem. Mol. Biol.* **82**, 31-40. doi:10.1016/j.ibmb.2017.01.009
- Woodbury, E. L. and Morgan, D. O.** (2007). Cdk and APC activities limit the spindle-stabilizing function of Fin1 to anaphase. *Nat. Cell Biol.* **9**, 106-112. doi:10.1038/ncb1523
- Wu, Z., Guo, W., Xie, Y. and Zhou, S.** (2016). Juvenile hormone activates the transcription of *cell-division-cycle 6 (Cdc6)* for polyploidy-dependent insect vitellogenesis and oogenesis. *J. Biol. Chem.* **291**, 5418-5427. doi:10.1074/jbc.M115.698936
- Wu, Z., Guo, W., Yang, L., He, Q. and Zhou, S.** (2018). Juvenile hormone promotes locust fat body cell polyploidization and vitellogenesis by activating the transcription of *Cdk6* and *E2f1*. *Insect Biochem. Mol. Biol.* **102**, 1-10. doi:10.1016/j.ibmb.2018.09.002
- Wyatt, G. R. and Davey, K. G.** (1996). Cellular and molecular actions of juvenile hormone II. Roles of juvenile hormone in adult insects. *Adv. In. Insect Phys.* **26**, 1-155. doi:10.1016/S0065-2806(08)60030-2
- Yadav, H., Devalaraja, S., Chung, S. T. and Rane, S. G.** (2017). TGF- β 1/Smad3 pathway targets PP2A-AMPK-FoxO1 signaling to regulate hepatic gluconeogenesis. *J. Biol. Chem.* **292**, 3420-3432. doi:10.1074/jbc.M116.764910
- Zeng, B., Huang, Y., Xu, J., Shiotsuki, T., Bai, H., Palli, S. R., Huang, Y. and Tan, A.** (2017). The FOXO transcription factor controls insect growth and development by regulating juvenile hormone degradation in the silkworm, *Bombyx mori*. *J. Biol. Chem.* **292**, 11659-11669. doi:10.1074/jbc.M117.777797
- Zhang, S., Guo, X., Chen, C., Chen, Y., Li, J., Sun, Y., Wu, C., Yang, Y., Jiang, C., Li, W. et al.** (2016). dFoxO promotes Wingless signaling in *Drosophila*. *Sci. Rep.* **6**, 22348. doi:10.1038/srep22348
- Zheng, H., Chen, C., Liu, C., Song, Q. and Zhou, S.** (2020). Rhythmic change of adipokinetic hormones diurnally regulates locust vitellogenesis and egg development. *Insect Mol. Biol.* **29**, 283-292. doi:10.1111/imb.12633
- Zielke, N., Edgar, B. A. and DePamphilis, M. L.** (2013). Endoreplication. *Cold Spring Harb. Perspect Biol.* **5**, a012948. doi:10.1101/cshperspect.a012948

Figure S1

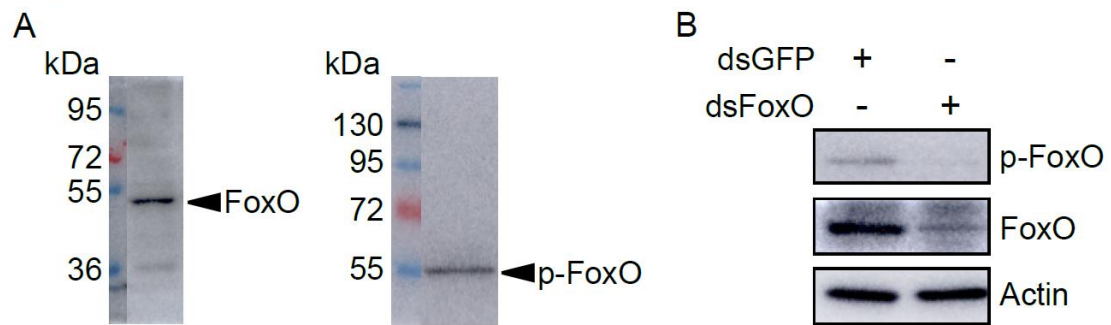


Fig. S1. Specificity of antibodies against FoxO and p-FoxO. (A) Western blots using protein extracts from the fat body of adult female locusts on day 8. Bands with various colors indicate the protein ladders labelled with respective molecular weights. The arrows indicate the predicted specific bands. (B) Western blots using protein extracts from the fat body of adult female locusts treated with dsFoxO vs. dsGFP controls.

Figure S2

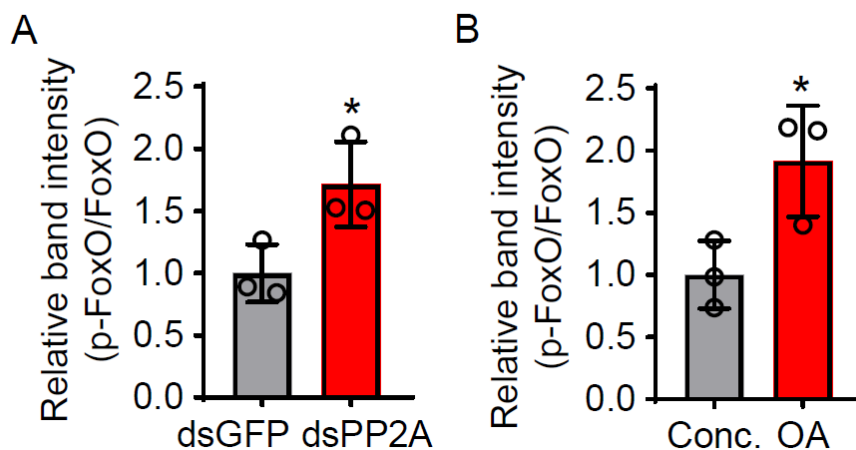


Fig. S2. Effect of PP2A knockdown and okadaic acid treatment on FoxO dephosphorylation. (A) Quantitative analysis by ImageJ of p-FoxO/FoxO band intensity in Western blots (represented by Fig. 2E) using protein extracts from the fat body of adult females subjected to dsPP2A and dsGFP treatment. *, $P < 0.05$ compared with the dsGFP controls. $n=3$. (B) Quantitative analysis by ImageJ of p-FoxO/FoxO band intensity in Western blots (represented by Fig. 2E) using protein extracts from the fat body of adult females treated with PP2A inhibitor, okadaic acid (OA) and solvent control, DMSO. *, $P < 0.05$ compared with the DMSO controls. $n=3$.

Figure S3

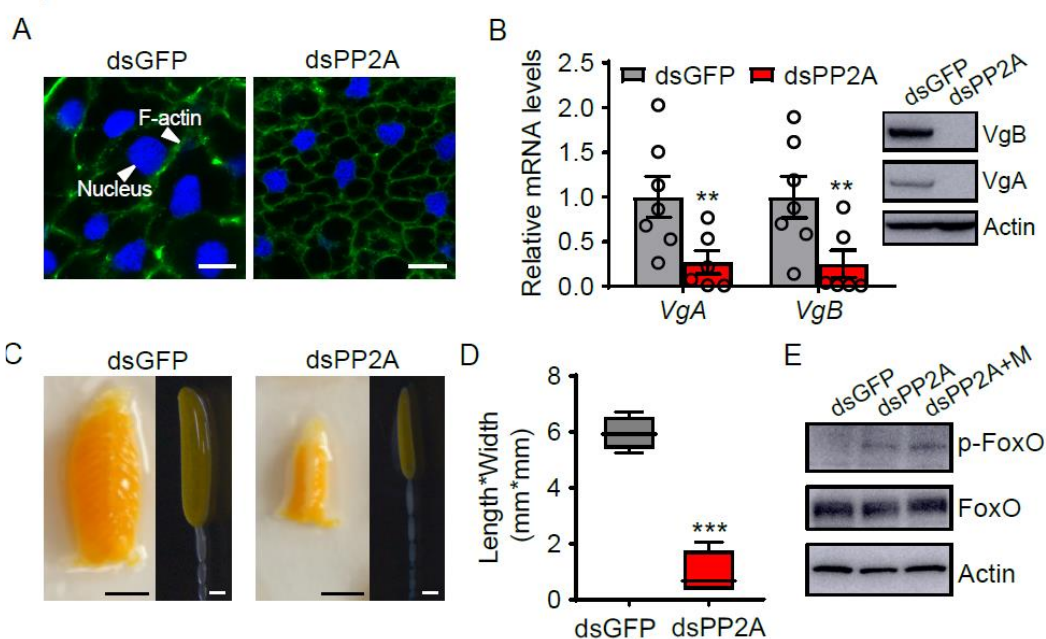


Fig. S3. Effect of *PP2A* knockdown on fat body cell ploidy, vitellogenesis and p-FoxO abundance. (A) Morphology change of fat body cells of adult females subjected to dsPP2A and dsGFP treatments on day 8. Blue, nuclei; green, F-actin. Scale bar, 20 μm . (B) Relative levels of *VgA* and *VgB* mRNA and protein in the fat body of dsPP2A-treated adult females vs. dsGFP controls on day 8. **, $P < 0.01$ compared to the respective dsGFP controls. $n = 6$. (C) Representative phenotypes of ovaries and primary oocytes subjected to dsPP2A treatment vs. dsGFP controls on day 8. Ov, ovary; Ol, ovariole; Po, primary oocyte. Scale bars: black, 5 mm; white, 0.5 mm. (D) Statistical analysis for length*width index of primary oocytes of dsPP2A- vs. dsGFP-treated adult females on day 8. ***, $P < 0.001$ compared with the dsGFP control. $n = 30$. (E) Relative abundance of FoxO and p-FoxO proteins in the fat body of adult females subjected to *PP2A* RNAi and those further treated with methoprene (dsPP2A+M).

Figure S4

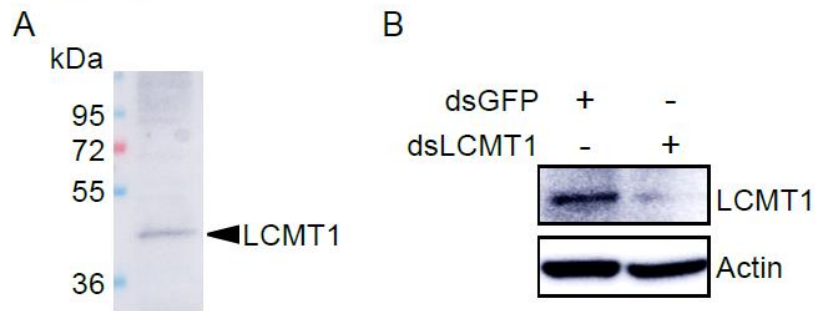


Fig. S4. Specificity of antibody against LCMT1. (A) Western blots using protein extracts from the fat body of adult females on day 8. Bands with various colors indicate the protein ladders labelled with respective molecular weight. The arrow indicates the predicted specific band. (B) Western blots using protein extracts from the fat body of adult females treated with dsFoxO vs. dsGFP controls.

Figure S5

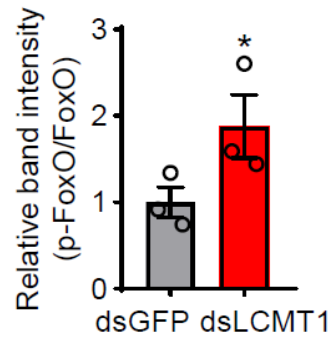


Fig. S5. Quantitative analysis of *LCMT1* RNAi effect on FoxO dephosphorylation.

Relative band intensity by ImageJ analysis for the ratio of p-FoxO/FoxO in Western blots (represented by Fig. 4D) using the protein extracts from the fat body of adult females treated with dsLCMT1 vs. dsGFP controls. *, $P < 0.05$ compared with the dsGFP control. n=3.

Figure S6

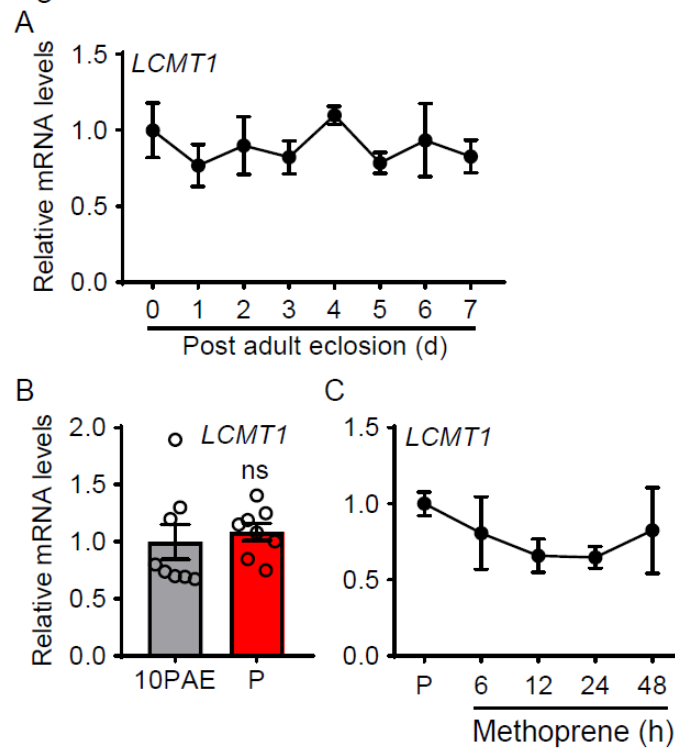


Fig. S6. *LCMT1* expression pattern and responsiveness to JH. (A) Developmental profile of *LCMT1* mRNA in the fat body adult females from 12 h after adult emergence (0 d) to 7 days (7 d) post adult eclosion. n=8. (B, C) Relative *LCMT1* mRNA levels in the fat body of 10-day-old adult females (10PAE), precocene-treated adult females for 10 days (P) and those further treated with methoprene for 6-48 h. ns, no significant difference. n=8.

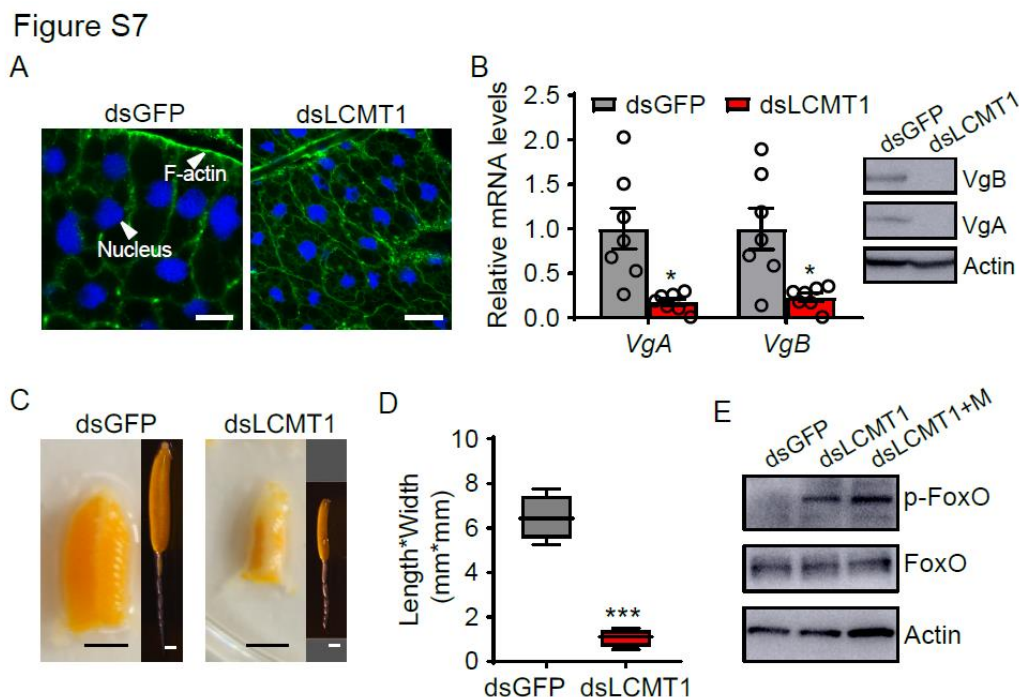


Fig. S7. Effect of *LCMT1* RNAi on fat body cell ploidy, vitellogenesis and p-FoxO abundance. (A) Morphology change of fat body cells of adult females after dsLCMT1 and dsGFP treatment on day 8. Blue, nuclei; green, F-actin. Scale bar, 20 μ m. (B) Relative levels of *VgA* and *VgB* mRNA and protein in the fat body of dsLCMT1-treated adult females vs. dsGFP controls on day 8. *, $P < 0.05$ compared to the respective dsGFP controls. $n = 6$. (C) Representative phenotypes of ovaries and primary oocytes subjected to dsLCMT1 treatment vs. dsGFP controls on day 8. Ov, ovary; Ol, ovariole; Po, primary oocyte. Scale bars: black, 5 mm; white, 0.5 mm. (D) Statistical analysis for length*width index of primary oocytes of dsLCMT1- and dsGFP-treated adult females on day 8. ***, $P < 0.001$ compared to the dsGFP control. $n = 30$. (E) Relative levels of FoxO and p-FoxO in the fat body of adult females subjected to *LCMT1* RNAi and those further treated with methoprene (dsLCMT1+M).

Figure S8

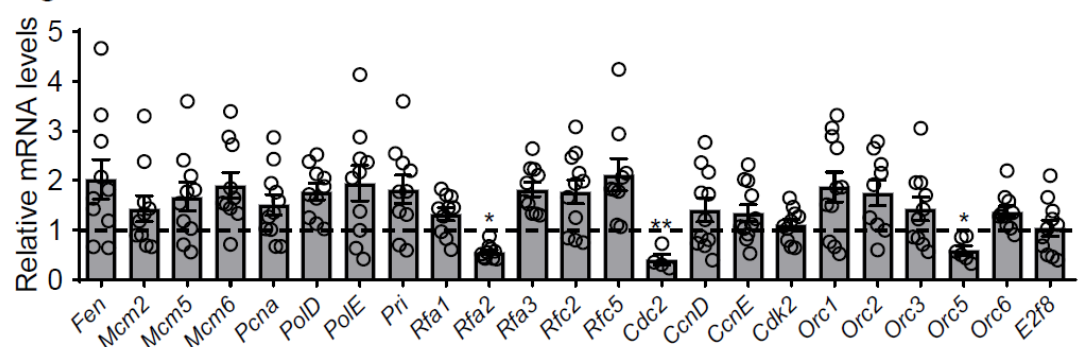


Fig. S8. Effect of *FoxO* knockdown on the expression of 23 genes associated with endocycle and polyploidization. *Fen*, Flap structure-specific endonuclease; *Mcm2*, 5 and 6: Chromosome maintenance 2, 5 and 6; *PcnA*: Proliferating cell nuclear antigen; *PolD*: DNA polymerase Delta; *PolE*: DNA polymerase Epsilon; *Pri*: DNA primase I; *Rfa1*, 2 and 3: Replication protein A1, 2 and 3; *Rfc2* and 5: Replication factor C subunit 2 and 5; *Cdc2*: cell-division-cycle 2; *CcnD*: Cyclin D; *CcnE*: Cyclin E; *Cdk2*: cyclin-dependent kinase 2; *Orc1*, 2, 3, 5 and 6: origin-recognition-complex subunit 1, 2, 3, 5 and 6; *E2f8*: adenovirus E2 factor-8. *, $P < 0.05$ and **, $P < 0.01$ compared to the dsGFP controls. $n=8$.

Table S1. Primers used for qRT-PCR, RNAi and antibody generation.

	Gene	Forward primer (5' to 3')	Reverse primer (5' to 3')
qRT-PCR	<i>FoxO</i>	TGTCCTACGCAGACCTCATC	GTCGCCCTTGTCCTTGAA
	<i>PP2A</i>	GCTGCTTGGTTCCCACAACG	CGCTGGTGTCTCGTGCTCAT
	<i>LCMT1</i>	TCGTTGTTTGTGCGCGGTAC	AGCGCCAGTACAATGTGTGCG
	<i>Cdc2</i>	GAGAAGGCACATATGGCGTTGT	GGTGAACCAGCTCTCGAAGAAG
	<i>Orc5</i>	GACTTGTAGGTCTGATTGGCC	TGCAGCTTGTTGAGTAGTTTTG
	<i>VgA</i>	CCCACAAGAAGCACAGAACG	TTGGTCGCCATCAACAGAAG
	<i>VgB</i>	AACGCCGACAGTGTTGGTATTC	ACCATCAGAAGTCGCTGGAAGT
	<i>Rp49</i>	CGTAAACCGAAGGGAATTGA	GAAGAACTGCATGGGCAAT
RNAi	<i>PP2A</i>	AGCTCCACGAGGCGATATGC	GGCCGCTCTCCAGACACAAA
	<i>LCMT1</i>	TTTGGGTTCTGGATTTCGACACA	TTCCTGCATGTAAATCAGTGGC
	<i>FoxO</i>	CCAGCTGGTGGATGATCAA	TTCATGCTCTCGGCTAGGT
	<i>Cdc2</i>	GCCGGGTGTTGCATAGAGA	AGTCCAGCCCATCATCATCA
	<i>Orc5</i>	AGGCAGCAATGAAGTGCAGT	CCAGGCTGCTCTTGAGGTGA
	<i>GFP</i>	CACAAGTTCAGCGTGTCCG	GTTACCTTGATGCCGTTT
Antibody	<i>FoxO</i>	AACTCGATCCGGCATAACC	GGTGGAGGGCCCGCTGGGC
	<i>LCMT1</i>	GAGAGAAAAGCACCTGAG	CATATTTACCTGTTCGTA